

**Title:** Spring Hydrology Determines Summer Net Carbon Uptake in Northern Ecosystems

Yonghong Yi<sup>1,2\*</sup>, John S. Kimball<sup>1,2</sup>, Rolf H. Reichle<sup>3</sup>

<sup>1</sup>Flathead Lake Biological Station, The University of Montana, 32125 Biostation Lane, Polson MT, USA, 59860-9659

<sup>2</sup>Numerical Terradynamic Simulation Group, The University of Montana, Missoula MT, USA, 59812

<sup>3</sup>Global Modeling and Assimilation Office, NASA Goddard Space Flight Center, Greenbelt, MD, USA, 20771

\*Corresponding Author Address: Yonghong Yi

Email: [yonghong.yi@ntsg.umt.edu](mailto:yonghong.yi@ntsg.umt.edu)

In preparation to submit to Environmental Research Letters.

## **Abstract**

Increased photosynthetic activity and enhanced seasonal CO<sub>2</sub> exchange of northern ecosystems have been observed from a variety of sources including satellite vegetation indices (such as the Normalized Difference Vegetation Index; NDVI) and atmospheric CO<sub>2</sub> measurements. Most of these changes have been attributed to strong warming trends in the northern high latitudes ( $\geq 50^{\circ}\text{N}$ ). Here we analyze the interannual variation of summer net carbon uptake derived from atmospheric CO<sub>2</sub> measurements and satellite NDVI in relation to surface meteorology from regional observational records. We find that increases in spring precipitation and snow pack promote summer net carbon uptake of northern ecosystems independent of air temperature effects. However, satellite NDVI measurements still show an overall benefit of summer photosynthetic activity from regional warming and limited impact of spring precipitation. This discrepancy is attributed to a similar response of photosynthesis and respiration to warming and thus reduced sensitivity of net ecosystem carbon uptake to temperature. Further analysis of boreal tower eddy covariance CO<sub>2</sub> flux measurements indicates that summer net carbon uptake is positively correlated with early growing-season surface soil moisture, which is also strongly affected by spring precipitation and snow pack based on analysis of satellite soil moisture retrievals. This is attributed to strong regulation of spring hydrology on soil respiration in relatively wet boreal and arctic ecosystems. These results document the important role of spring hydrology in determining summer net carbon uptake and contrast with prevailing assumptions of dominant cold temperature limitations to high-latitude ecosystems. Our results indicate potentially stronger coupling of boreal/arctic water and carbon cycles with continued regional warming trends.

**Keywords:** boreal, arctic, productivity, respiration, net carbon uptake, spring hydrology, soil moisture

## 1. Introduction

Northern boreal and arctic ecosystems are an important component of the global carbon cycle, and their sensitivity to climate change remains largely uncertain (McGuire *et al* 2012). Besides a strong warming trend in the northern high latitudes ( $\geq 50^\circ\text{N}$ ), an increase in spring precipitation is also likely to occur (Solomon *et al* 2007), which might have a profound impact on regional ecosystems and the carbon cycle, including photosynthesis, soil litter decomposition and respiration, and disturbance (e.g. fire, insects). Previous studies have largely focused on how warming affects vegetation growth and associated carbon ( $\text{CO}_2$ ) uptake (Angert *et al* 2005, Piao *et al* 2008, Zhang *et al* 2008, Xu *et al* 2013), while few studies have addressed how variations in seasonal precipitation and temperature together affect surface hydrology and its impact on net ecosystem carbon uptake of northern ecosystems. Vegetation greening and increasing carbon uptake associated with warming in the spring have been observed at both field and large ecosystem scales indicated by satellite greenness indices, atmospheric  $\text{CO}_2$  seasonal cycles and in situ tower eddy covariance  $\text{CO}_2$  flux measurements (Nemani *et al* 2003, Welp *et al* 2007, Beck and Goetz 2011, Graven *et al* 2013, Xu *et al* 2013). However, how northern vegetation responds to temperature increases in the summer is uncertain, with both vegetation greening and browning being reported from satellite vegetation indices and similar conflicting findings reported from tower eddy covariance measurements (Angert *et al* 2005, Welp *et al* 2007, Zhang *et al* 2008, Buermann *et al* 2013). A few field studies have shown that surface and subsurface hydrology have a dominant role in regulating the interannual variation of net carbon uptake in both boreal and arctic ecosystems (Desai *et al* 2010, Olivas *et al* 2010, Lupascu *et al* 2013);

however, these relatively scarce and short-duration measurements may not be representative of how net ecosystem carbon uptake responds to changes in surface hydrology at regional scales.

The objective of this study is to investigate how spring hydrology and summer temperature affect the interannual variability of summer vegetation growth and regional net carbon (CO<sub>2</sub>) uptake in the northern high latitudes ( $\geq 50^\circ\text{N}$ ). To that end, we conducted a synthesized analysis of atmospheric CO<sub>2</sub> observations, net ecosystem exchange (NEE) CO<sub>2</sub> fluxes simulated by a global atmospheric Bayesian model inversion system, satellite NDVI (Normalized Difference Vegetation Index) measurements over the past 3 decades (from 1979), and more recent tower eddy covariance measured carbon fluxes and satellite surface soil moisture retrievals (2003-2011).

## **2. Methods and Datasets**

The seasonal cycle of atmospheric CO<sub>2</sub> in the northern high latitudes is primarily driven by the net ecosystem productivity (NEP) of underlying terrestrial ecosystems (Randerson *et al* 1997). The atmospheric CO<sub>2</sub> seasonal cycle ( $\geq 50^\circ\text{N}$ ) was derived from Marine Boundary Layer (MBL) Reference data available from the National Oceanic and Atmospheric Administration (NOAA) Earth System Research Laboratory (ESRL), which was based on measurements from a subset of sites from the NOAA Cooperative Global Air Sampling Network representing well-mixed MBL air samples of a large volume of atmosphere (Masarie *et al* 1995). The detrended atmospheric CO<sub>2</sub> seasonal cycle was first extracted from the weekly CO<sub>2</sub> concentration records following Thoning *et al* (1989). Generally, for the northern high latitudes, the spring zero-crossing time of the mean CO<sub>2</sub> seasonal cycle occurs at the end of June, and reaches a minimum at the end of August. This CO<sub>2</sub> minimum (CO<sub>2</sub>\_sum\_min) was then used as a surrogate of the net carbon uptake occurring from June to August (Angert *et al* 2005). In addition, the CO<sub>2</sub> seasonal cycle

was also extracted from weekly atmospheric CO<sub>2</sub> measurements at 9 northern ( $\geq 50^\circ\text{N}$ ) MBL flask sites (Table S1) obtained from the ESRL GLOBVIEW-CO<sub>2</sub> dataset.

We also examined the CO<sub>2</sub> seasonal cycle of northern ecosystems simulated by two global atmospheric inversion models, including a Bayesian inversion system (Chevallier *et al* 2010; available from 1979 to 2011) and CarbonTracker (Peters *et al* 2007; available from 2000 to 2010). For the long-term Bayesian inversion system, surface CO<sub>2</sub> mixing ratio measurements from more than 128 stations were assimilated within a Bayesian system framework and a Monte Carlo approach was used to estimate the error statistics of the inverted fluxes. The surface fluxes were simulated on a  $3.75^\circ \times 2.5^\circ$  (longitude-latitude) grid. The simulated zonal-averaged ( $\geq 50^\circ\text{N}$ ) monthly NEE fluxes were used to analyze the relations between climate controls and northern summer carbon uptake for the past 3 decades. The CarbonTracker data assimilation system uses the atmospheric Transport Model 5 (TM5) and an ensemble Kalman filter to reanalyze the recent flux history of CO<sub>2</sub> with ingestion of global observations of atmospheric CO<sub>2</sub> mole fractions. The CO<sub>2</sub> mole fraction distributions simulated by CarbonTracker were used to analyze the contribution of each component flux including fossil fuel emissions, NEE, fire emissions and air-sea gas exchange contributions to the northern atmospheric CO<sub>2</sub> seasonal cycle. The CO<sub>2</sub> mole fractions were simulated on a  $3^\circ \times 2^\circ$  (longitude-latitude) grid.

Satellite vegetation greenness indices like the NDVI have been widely used as a surrogate of vegetation gross primary productivity (e.g. Beck and Goetz 2011, Buermann *et al* 2013, Xu *et al* 2013). A long-term global 8-km bimonthly satellite NDVI dataset (1982-2010) was obtained from the third-generation Global Inventory Monitoring and Modelling Studies (GIMMS3g) dataset (Xu *et al* 2013). This dataset was assembled from different NOAA Advanced Very High Resolution Radiometer (AVHRR) sensor records, accounting for various deleterious effects

including calibration loss, orbital drift and volcanic eruptions. For this analysis, the GIMMS3g data were aggregated to 0.5° spatial resolution and monthly temporal resolution. Fire emission is also a large component of the boreal carbon cycle (Bond-Lamberty *et al* 2007). Monthly CO<sub>2</sub> fire emissions from 1997 to 2011 were obtained from the Global annual Fire Emission Database version 3 (GFED v.3.1); fire emissions were generated using a revised Carnegie-Ames-Stanford-Approach (CASA) biogeochemical model and improved satellite-derived estimates of burned areas, fire activity and plant productivity at 0.5° spatial resolution with a monthly time step (van der Werf *et al* 2010). The GFED dataset indicates that on average around 70% of fire CO<sub>2</sub> emissions in areas north of 50 °N occurs during the period from June to August.

Climate records used in this study include surface air temperature (T) from the 0.5° CRU (Climate Research Unit) TS3.20 datasets (Harris *et al* 2013), precipitation (P) from GPCP (Global Precipitation Climatology Project, version 2.2) 2.5° gridded data (Adler *et al* 2012), and snow water equivalent (SWE) from the Canadian Meteorological Center (CMC) snow depth analysis (Brown and Brasnett 2010). The CRU dataset is based on climate observations from more than 4000 weather stations around the globe. The GPCP dataset is a merged product combining observations from over 6000 rain gauge stations with rainfall estimates from satellite geostationary and low-orbit infrared, passive microwave and sounding observations. The CMC snow depth analysis merges surface synoptic observations, meteorological aviation reports, and special aviation reports with snow model estimates. SWE is estimated from the snow depth analysis using a snow density look-up table. The CMC data are available from August 1998 to December 2012 at a 24-km resolution polar stereographic grid. Both the GPCP precipitation and CMC SWE data were interpolated to 0.5° spatial resolution prior to the analysis.

We tested the dependence of the carbon indices, including NDVI, CO<sub>2</sub>\_sum\_min, fire emission and model inversion NEE fluxes, on the seasonal climate variables including T, P, and SWE using partial correlation analysis, which was used to account for the co-variation of these climate variables. Our analysis focused on vegetated areas defined by the MODIS 500-m global land cover map (MCD12Q1; Friedl *et al* 2010) and all time series were detrended to focus on the co-variation of annual anomalies of the climate and vegetation parameters.

Measurements from approximately 23 northern ( $\geq 50^\circ\text{N}$ ) eddy covariance (EC) flux towers (Table S2) with two or more years of measurements covering at least part of the growing season (May-August) were obtained from the global FLUXNET dataset (Baldocchi 2008); these data were used to analyze local scale relations between summer net carbon uptake and climate variability. The tower daily carbon flux estimates are derived from half-hourly EC CO<sub>2</sub> flux measurements that have been processed and aggregated using consistent gap filling and quality control procedures. Temporal anomalies of summer net carbon uptake at each site are simply the difference of monthly aggregated NEE fluxes from June to August from the multi-year ( $\geq 2$  years) means.

Daily satellite surface soil moisture retrievals were obtained from an AMSR-E (Advanced Microwave Scanning Radiometer for EOS) global land parameter database developed at the University of Montana for ecosystem studies (Jones and Kimball 2010); these data were used to analyze how seasonal climate variations affect surface soil moisture. The soil moisture retrievals were generated at 6.9 GHz and 10.7 GHz wavelengths using an iterative radiative transfer algorithm and multi-frequency AMSR-E brightness temperature inputs under non-precipitating and snow/ice-free conditions (Jones *et al* 2007). The radiative transfer algorithm accounts for surface emissivity variations caused by vegetation roughness and inland and coastal water bodies,

which may have a large influence on soil moisture retrievals in the northern high latitudes (Yi *et al* 2011). The AMSR-E soil moisture retrievals are available at 25 km resolution and daily time step from 2003 to 2011. Monthly averaged soil moisture was calculated when there were more than 5 daily retrievals within a given month.

### **3. Results**

#### **3.1 Summer net CO<sub>2</sub> uptake and associated climate controls**

The interannual variations of detrended summer (JJA, from June to August) net CO<sub>2</sub> uptake derived from the MBL atmospheric CO<sub>2</sub> data and spring (MAM, from March to May) precipitation for the zone north of 50°N are shown in Fig. 1 (a). The results suggest that interannual variations of spring precipitation play an important role in controlling interannual variations of summer net carbon uptake, with large spring precipitation anomalies generally associated with strong summer net carbon uptake in the northern high latitudes. Significant negative correlation ( $R=-0.55$ ,  $p<0.001$ ) was found between the detrended time series of spring precipitation and summer net carbon uptake (Fig. 1b). A weak negative correlation ( $R=-0.35$ ,  $n=13$ ,  $p>0.1$ ) was also found between summer net carbon uptake and spring snow water equivalent (SWE) (Fig. 1b). Summer air temperature (T) appears to have only a minimal impact on summer net carbon uptake. Further analysis (Table S3) indicates that summer net carbon uptake is most strongly correlated with winter and spring precipitation (from January to May,  $R=-0.57$ ,  $p<0.001$ ) and peak winter SWE (February,  $R=-0.51$ ,  $n=13$ ,  $p<0.1$ ). The results based on atmospheric CO<sub>2</sub> measurements at the northern ( $\geq 50^\circ\text{N}$ ) flask sites were generally similar to the results based on the MBL reference datasets (Fig. 1b).

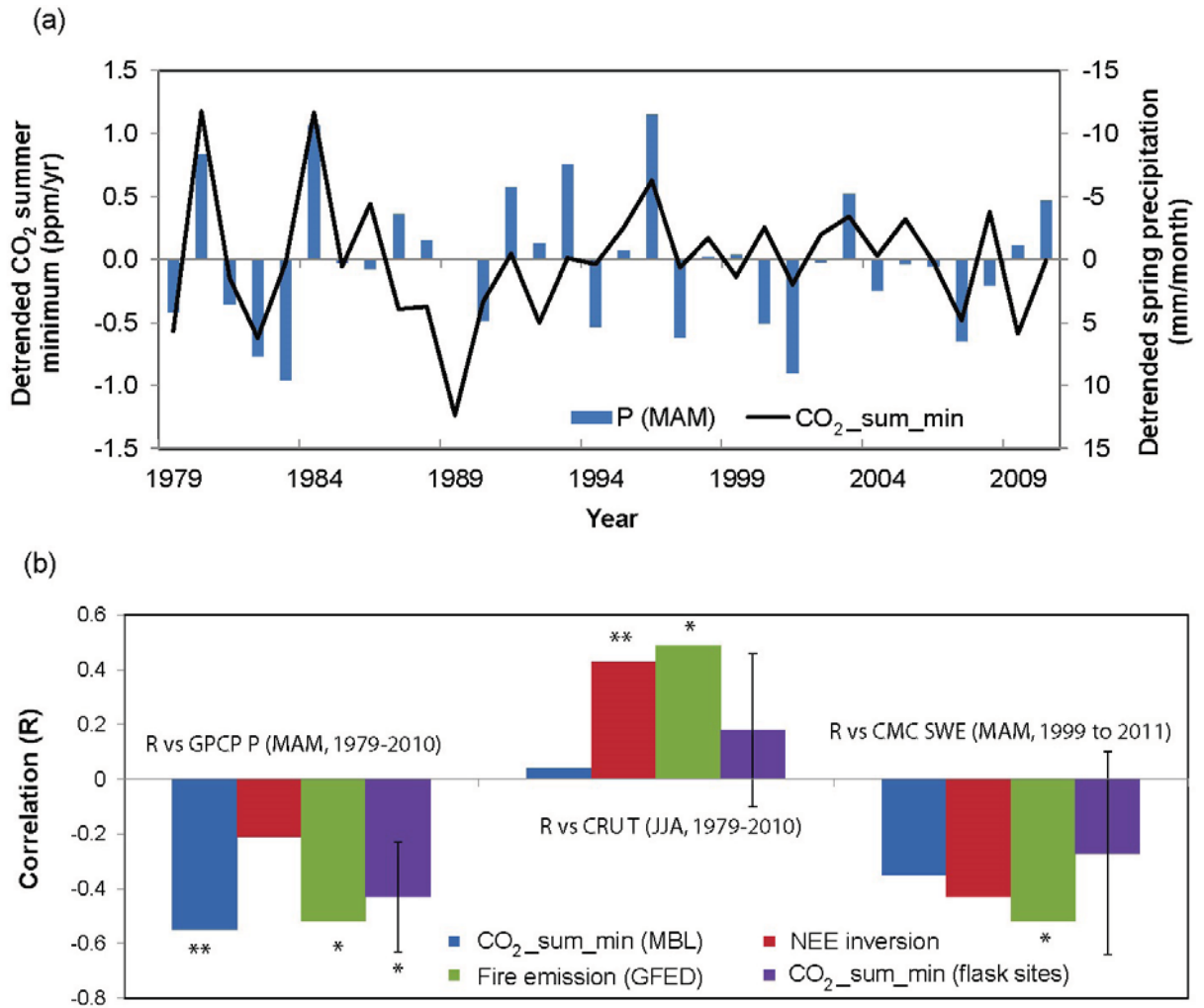


**Fig. 1.** Co-variation of summer net carbon uptake and climate variables. (a) Time series of detrended summer CO<sub>2</sub> minimum (CO<sub>2</sub>\_sum\_min) derived from NOAA MBL reference data and GPCP spring (MAM) precipitation (P) averaged for zone 50 °N to 90 °N, where positive (negative) anomalies denote relative decreases (increases) in terrestrial carbon uptake. (b) Partial correlation (R) analysis of carbon fluxes including CO<sub>2</sub>\_sum\_min, global atmospheric inversion model estimated NEE fluxes (Chevallier *et al* 2010), and GFED (v.3.1) estimated CO<sub>2</sub> fire emissions versus seasonal climate variables. The CO<sub>2</sub>\_sum\_min values derived from atmospheric CO<sub>2</sub> records from both MBL reference datasets and northern ( $\geq 50$  °N) CO<sub>2</sub> flask monitoring sites (Table S1) were used. The error bars represent the standard deviation of R values for the 9 flask sites. For the partial correlation analysis against P and SWE, T was used as the controlling variable, while P was used as the controlling variable for the partial analysis

against T. All time series were detrended prior to the temporal correlation analysis; asterisks \*\* and \* denote statistical significance at 95% ( $p < 0.05$ ) and 90% ( $p < 0.1$ ) levels, respectively.

The summer NEE fluxes derived from the global atmospheric Bayesian inversion system (Chevallier *et al* 2010) showed a strong positive correlation with summer air temperature ( $R=0.43$ ,  $p < 0.05$ ), and a weak negative correlation with spring precipitation ( $R=-0.21$ ,  $p > 0.1$ ), and SWE ( $R=-0.43$ ,  $n=13$ ,  $p > 0.1$ ), as shown by the red bars in Fig. 1b. Further analysis (Table S3) indicates that the model inversion summer NEE fluxes are most positively correlated with mid-summer air temperature (from July to August,  $R=0.52$ ,  $p < 0.05$ ), and most negatively correlated with precipitation during winter and early spring (from February to April,  $R=-0.33$ ,  $p < 0.1$ ), and SWE during later spring (from April to May,  $R=-0.51$ ,  $n=13$ ,  $p < 0.1$ ).

The difference between the results based on the atmospheric CO<sub>2</sub> seasonal cycle and model inversions may be partly due to the variation of atmospheric transport from year to year and its impact on the atmospheric CO<sub>2</sub> seasonal cycle, though this impact is relatively small (generally less than 10-15%; Piao *et al* 2008, Graven *et al* 2013) compared to characteristic large variations in the northern CO<sub>2</sub> seasonal cycle. On the other hand, current atmospheric inversion models still have difficulty in clearly distinguishing regional carbon budgets within a continent (Chevallier *et al* 2010, Gurney *et al* 2008), and may not be able to accurately distinguish carbon uptake patterns between the northern middle and high latitudes.

In the high latitudes, fire emissions generally peak in the summer and also contribute to the variation of the atmospheric CO<sub>2</sub> seasonal cycle. Large fire emissions generally correspond with reduced summer carbon uptake indicated by both model inversions and atmospheric CO<sub>2</sub> data (Fig. S1). Partial correlation analysis indicates that summer air temperature ( $R=0.49$ ,  $n=14$ ,  $p < 0.1$ ) and spring hydrology (for MAM P,  $R=-0.52$ ,  $n=14$ ,  $p < 0.1$ ; for MAM SWE,  $R=-0.52$ ,

n=13,  $p<0.1$ ) are the two major climatic factors controlling interannual variability of fire emissions in the northern latitudes.

### 3.2 Summer NDVI and associated climate controls

The spatial distribution of partial correlation coefficients between detrended satellite-derived summer NDVI and summer T or spring P in the northern latitudes ( $\geq 50^\circ\text{N}$ ) is shown in Fig. 2. Summer NDVI is strongly positively correlated with summer (JJA) T (Fig. 2a). This is especially true for early summer (June) temperature (Fig. S2). Moreover, correlations are generally higher for tundra than boreal forest areas (Fig. 2c). Around 60.5%, 23.7% and 21.0% of tundra areas show significant ( $p<0.1$ ) positive NDVI correlation with respective June, July and August air temperatures, while only 29.4%, 13.1% and 14.4% of boreal forest areas show significant positive correlation for these months (Fig. S2). On the other hand, summer NDVI is much more weakly correlated with spring P (Fig. 2b), with 12.5% of boreal forest areas and 2.9% of tundra areas showing significant positive correlation (Fig. 2d). Similarly, a small portion (7.3%) of boreal forest areas show significant positive correlation between summer NDVI and early spring (from March to April) SWE, while a relatively larger portion (13.0%) of tundra areas show significant negative correlation between summer NDVI and later spring (May) SWE (not shown).

These results indicate that regional warming still promotes vegetation growth, especially in tundra areas. However, the relative benefits of summer warming are lower for boreal forest than tundra ecosystems, while summer NDVI is even negatively correlated with summer air temperature (Fig. 2a) in some areas subjected to frequent disturbance, e.g. western North America (Kurz *et al* 2008). Stronger positive correlations between summer NDVI and spring P and SWE in boreal forest are consistent with previous studies reporting greater summer water stress in boreal forest than tundra ecosystems (Zhang *et al* 2008, Beck and Goetz 2011,

Buermann *et al* 2013, Xu *et al* 2013). A negative correlation between summer NDVI and May SWE in tundra areas is likely due to a delayed onset of spring growth for years with a larger spring snow pack.

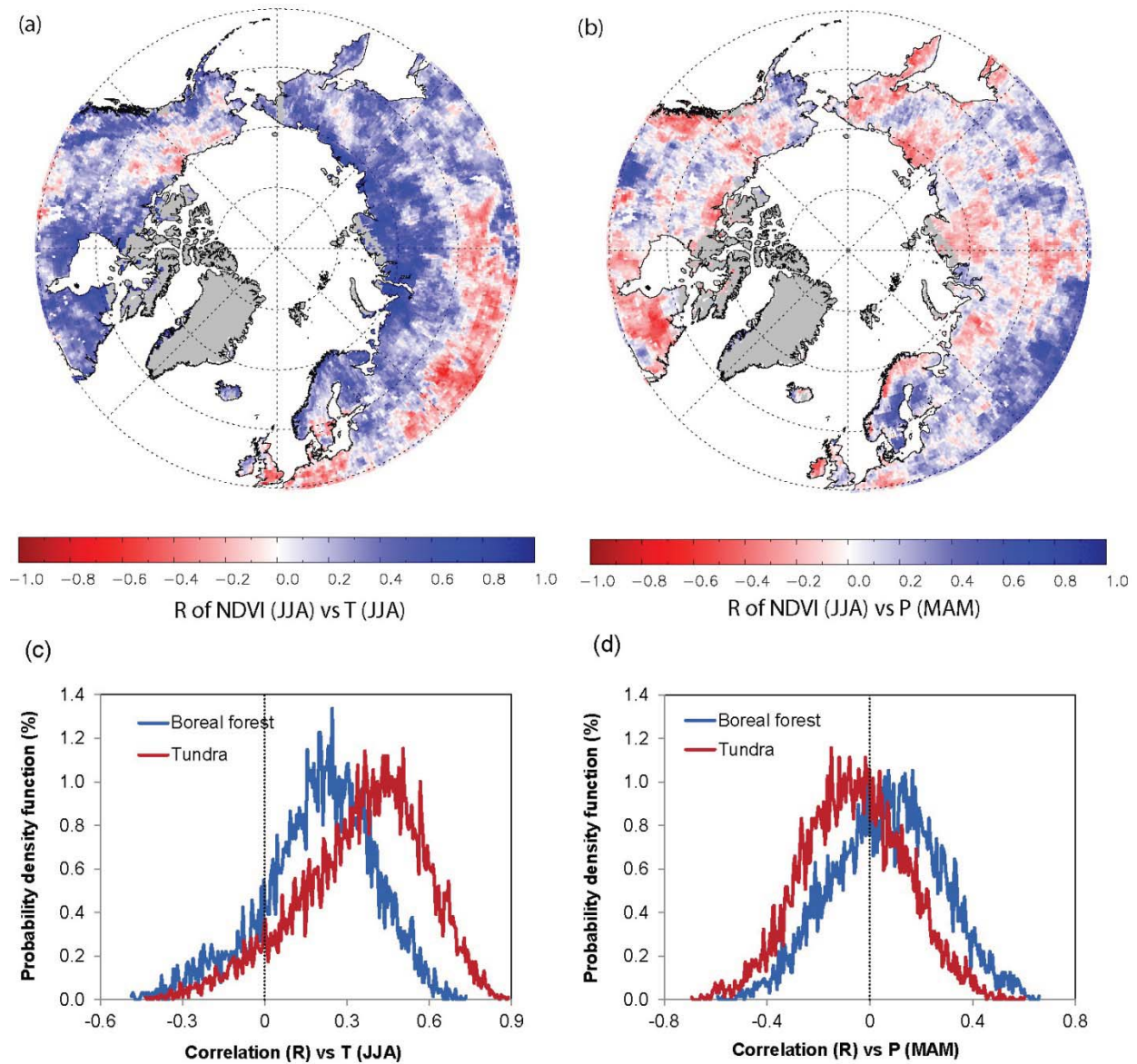


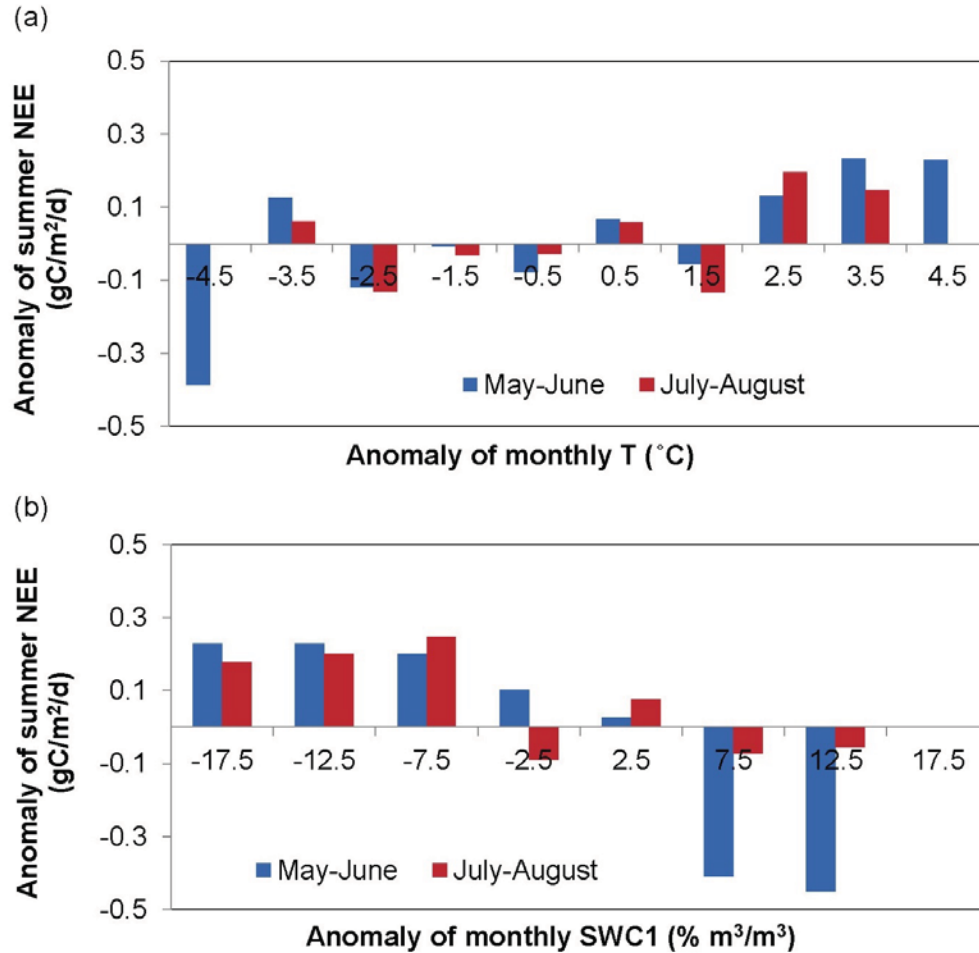
**Fig. 2.** Sensitivity of summer NDVI changes, used as a surrogate for vegetation growth, to climate variation in the northern latitudes ( $\geq 50^\circ\text{N}$ ). Maps (a) & (b) show partial correlation (R) patterns between summer (JJA) NDVI (GIMMS3g) anomalies versus summer air temperature (T, CRU) controlled by

precipitation (P, GPCP) and spring (MAM) P controlled by T over the 1982 to 2010 NDVI record; areas in gray denote regions with missing data or non-vegetated areas. Plots (c) & (d) show probability density functions of the above correlation coefficients for tundra and boreal forest areas of the northern domain. For boreal forest, 29.2% and 12.5% of the pixels show significant ( $p < 0.1$ ) positive correlation with T (JJA) and P (MAM) respectively. For tundra, 61.3% and 2.9% of the pixels show significant positive correlation with T (JJA) and P (MAM). All time series were detrended prior to the temporal correlation analysis.

A larger impact of spring P and SWE on summer net carbon uptake than on summer NDVI indicates that low spring P or snow pack together with high summer T may promote fire emissions and ecosystem respiration, which may offset the relative benefits of warming on photosynthesis, and dominate the signal shown in the atmospheric CO<sub>2</sub> seasonal cycle. The NOAA ESRL CarbonTracker carbon flux inversions from 2000 to 2010 also indicate a much smaller contribution of summer fire emissions (and also other carbon fluxes including fossil fuel emissions and air-sea gas exchange) to the interannual variability of summer atmosphere CO<sub>2</sub> minimums relative to terrestrial NEE contributions (Fig. S3), consistent with Wunch *et al* (2013). Therefore, the strong influence of spring P or snow (SWE) on summer net carbon uptake should mainly reflect the impact of spring hydrology on ecosystem respiration in relatively wet boreal and arctic regions, while a similar response of photosynthesis and respiration to temperature may reduce the apparent sensitivity of the residual NEE carbon flux to temperature variability (Yi *et al* 2013).

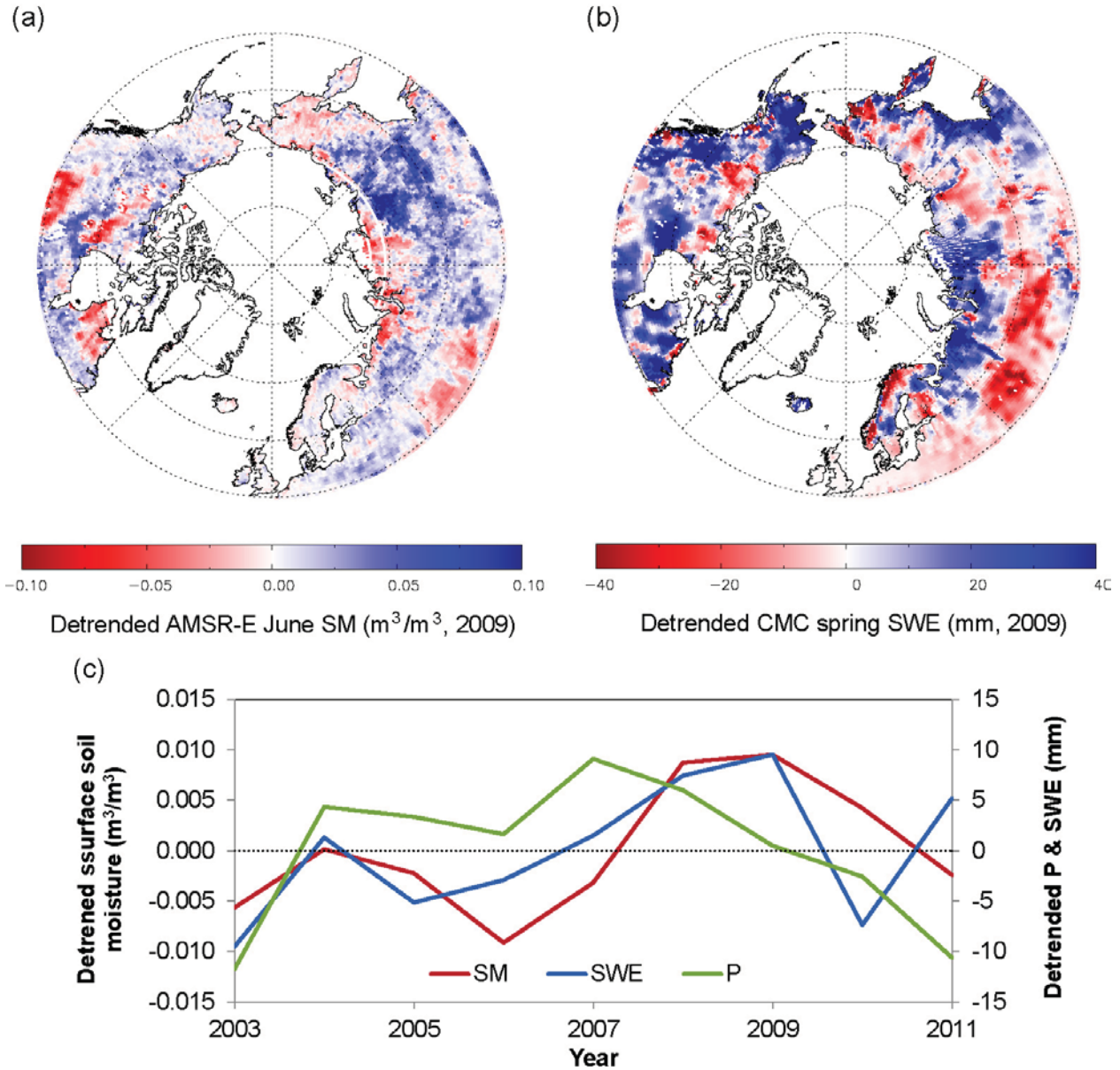
### **3.3 Summer NEE and spring hydrology**

Fig. 3 shows the anomalies of observed summer (JJA) NEE versus anomalies of monthly average T (Fig. 3a) and surface ( $\leq 15$  cm) soil water content (SWC1) (Fig. 3b) during the growing season (from May to August) from 23 boreal ( $\geq 50^\circ\text{N}$ ) EC tower sites in North America and northern Eurasia (Table S2). These results indicate that boreal ecosystems tend to lose carbon under relative warm or dry conditions. Summer NEE is generally positively correlated with growing-season T, and negatively correlated with growing-season SWC1 especially during the early growing season (from May to June, Table S4). However, the correlation between summer NEE and SWC1 may be caused by co-variation of SWC1 and T. To examine this, we also looked at the correlation of monthly SWC1 and T anomalies. SWC1 only shows a marginal correlation with T during the growing season (Table S4) except for April, when a strong positive correlation between T and SWC1 is found ( $R=0.72$ ,  $p<0.001$ ). A positive correlation between SWC1 and T in April and May is coincident with spring snowmelt and soil thawing, while SWC1 becomes more negatively correlated with T during the later growing season (July and August), likely due to more evaporation and associated soil water loss in the later season. Therefore, a consistent negative correlation between summer NEE and growing-season SWC1 is not likely due to the co-variation between T and SWC1 during this period.



**Fig. 3.** Tower EC data analysis for boreal NA and Northern Eurasian sites. The temporal anomalies of tower measured summer (JJA) NEE fluxes are shown against (a) monthly air temperature anomalies binned into 1.0 °C intervals, and (b) surface ( $\leq 15$  cm) soil water content (SWC1) anomalies binned into 0.05  $\text{m}^3/\text{m}^3$  intervals. For the air temperature analysis, there are 48, 48, 48, and 49 site-years used to represent each month from May to August, respectively; for soil moisture, there are 29, 26, 23, and 28 site-years used to represent each month from May to August. The analysis period is divided into early growing-season (May-June) and later growing-season (July-August) periods. Positive (negative) NEE anomalies denote relative reductions (increases) in terrestrial carbon uptake.

Further analysis using the satellite-derived (AMSR-E) surface ( $\leq 2$  cm) soil moisture record indicates that soil moisture is closely associated with spring hydrology during the early growing season (June, Fig. 4), but more strongly impacted by T during the later growing season (July and August, not shown). A larger spring snow pack is generally associated with higher surface soil moisture during the early growing season (Fig. S5 & Fig. S6), with some exceptions (e.g. year 2010) where the surface soil moisture is more closely associated with spring precipitation. The AMSR-E soil moisture for May is not shown due to screening of persistent ice/snow cover and frozen soil conditions in most tundra areas, but is generally similar to the June soil moisture pattern. During the later growing season, the AMSR-E soil moisture record becomes more negatively correlated with T (July and August, mean  $R=-0.14$ ; with 14.6% pixels showing significant correlation) than during the early season (May and June, mean  $R=-0.08$ ; with 13.4% pixels showing significant correlation). These regional results are generally consistent with the local tower EC based analysis. However, it should be noted that the satellite-derived soil moisture retrievals are associated with large uncertainties, especially during the peak growing season with high aboveground biomass and extensive surface open water, and these data should be interpreted with caution (Jones *et al* 2007, Yi *et al* 2011).



**Fig. 4.** Co-variation of AMSR-E retrieved surface ( $\leq 2$ cm) soil moisture in June and spring hydrology (P & SWE). The spatial patterns of detrended AMSR-E soil moisture in June (a) and CMC spring (MAM) SWE (b) for a particularly wet year (2009) are shown. The detrended time series (2003-2011) of regional mean AMSR-E June soil moisture (SM), spring CMC SWE and GPCP P are shown in (c). Large spring precipitation or snow pack anomalies generally correspond with large surface soil moisture in June.

#### 4. Discussion

Our results indicate that spring hydrology is an important climatic factor determining summer net carbon uptake in the northern high latitudes, and it is likely to have an increasing impact on the boreal/arctic carbon cycle given projected increases in regional temperatures and cold season precipitation. Air temperature is generally considered to be the dominant climatic factor controlling carbon uptake in boreal and arctic ecosystems (Piao *et al* 2008, Yi *et al* 2010, Kim *et al* 2012). However, because photosynthesis and respiration may respond similarly to warming in the northern latitudes, the sensitivity of NEE to temperature may be reduced (Yi *et al* 2013); these parameters may also respond differently to soil water conditions. Boreal and arctic soils are generally wet and poorly drained, with relatively cold temperatures that are a strong constraint to soil respiration (Davidson *et al* 1998, Goulden *et al* 1998). A few field studies in boreal forest and tundra ecosystems have demonstrated that local water table depth and surface hydrology strongly influence interannual variability of net ecosystem carbon uptake (Desai *et al* 2010, Olivas *et al* 2010, Lupascu *et al* 2013). The present study provides similar evidence of the important role of surface hydrology on the net carbon uptake of northern ecosystems at a regional scale. However, local conditions may also play a role in the integrated regional ecosystem response to climate variations. For example, summer carbon uptake has been found to increase with temperature warming at a few boreal sites in northern Europe (Fig. S4 and Table S5), where soil and forest conditions may be quite different from boreal North America and Russia (Valentini *et al* 2000).

Our analysis of the atmospheric CO<sub>2</sub> observations assumes that northern terrestrial ecosystems have a dominant influence on the CO<sub>2</sub> seasonal cycle above 50°N, while other studies have demonstrated that mid-latitude temperate ecosystems can also have a sizable influence on the northern atmospheric CO<sub>2</sub> seasonal cycle (e.g. Randerson *et al* 1997, Graven *et*

*al* 2013, Wunch *et al* 2013). The study of Wunch *et al* (2013) indicated covariance of column-averaged summer CO<sub>2</sub> minimums from Northern Hemisphere TCCON (Total Carbon Column Observing Network) and GOSAT (Greenhouse gases Observing SATellite) observations, and August temperatures averaged from zone 30°N to 60°N. The relatively strong correspondence between summer T and atmosphere CO<sub>2</sub> indicated from Wunch *et al.* (2013) is likely due to large-scale temperature-related atmosphere dynamical mixing and relative strong sensitivity of ecosystem summer carbon uptake to temperature and drought in the mid-latitudes, especially during the later growing season (Angert *et al* 2005, Piao *et al* 2008, Yi *et al* 2010). Underestimated seasonality of fossil fuel emissions (Gurney *et al* 2005) and increasing northern energy development during the last decade may also influence the atmospheric CO<sub>2</sub> seasonal cycle, though our analysis of CarbonTracker simulations from 2000 to 2010 showed a relatively small impact of fossil fuel emissions relative to terrestrial ecosystems during that period (Fig. S3). On the other hand, the Bayesian atmospheric inversion model analysis indicates a large impact of summer temperature on the net carbon uptake of northern ecosystems compared to a negligible summer temperature influence on the northern atmospheric CO<sub>2</sub> summer minimum. However, atmospheric inversion models generally have difficulties in locating a carbon sink within a continent due to sparse atmospheric CO<sub>2</sub> observations and large uncertainties in atmospheric transport modeling (Gurney *et al* 2008).

Besides precipitation, regional estimation of snow and soil moisture has large uncertainties in the northern high latitudes due to sparse weather station networks, difficulties in measuring snowfall with gauges, and relatively lower accuracy in satellite-based precipitation, snow and soil moisture retrievals in those areas (e.g. Adler *et al* 2012, Dong *et al* 2005, Yi *et al* 2011). A set of new NASA hydrology missions, including SMAP (Soil Moisture Active and Passive,

Entekhabi *et al* 2010) and GPM (Global Precipitation Measurement, Smith *et al* 2007), are expected to provide global measurements of surface ( $\leq 5\text{cm}$ ) soil moisture and precipitation with improved accuracy and spatial resolution (less than 10km); the Orbiting Carbon Observatory (OCO)-2 is designed to collect global measurements of vertical atmospheric CO<sub>2</sub> profiles at much higher resolution and precision than current sparse atmospheric observation networks (Boesch *et al* 2011). These new observational capabilities are expected to enable improved regional estimates of CO<sub>2</sub> sources and sinks, and their associated climate sensitivity.

## **5. Conclusions**

Our work illuminates the important role of spring hydrology in determining summer net carbon uptake even in predominantly temperature-limited high-latitude ecosystems. Large precipitation or snow cover conditions in spring generally promote summer net carbon uptake independent of air temperature effects as indicated by both the atmospheric CO<sub>2</sub> seasonal cycle and tower EC measurements. In contrast, satellite NDVI measurements still indicate an overall benefit of summer vegetation growth from warming. This discrepancy is attributed to a similar response of photosynthesis and respiration to temperature, resulting in reduced temperature sensitivity of the residual net carbon flux. On the other hand, spring precipitation and snow cover are closely related to surface soil moisture during the early growing season, exerting a strong control on soil respiration in relatively wet boreal and arctic ecosystems. Spring precipitation also strongly regulates summer fire emissions in the high latitudes, which may become more important to the regional carbon budget with continued warming. Spring hydrology is therefore likely to have an increasing impact on the northern carbon cycle under current climate trends and projections of increasing cold season precipitation and magnified warming trends over the northern high latitudes. If current warming trends continue, the regional carbon and water cycles may become

more closely coupled as northern ecosystems switch from primarily energy limited to stronger water limitations for vegetation growth and carbon sink activity.

**ACKNOWLEDGMENTS.** This study used eddy covariance data acquired by the FLUXNET community, which was supported by the CarboEuropeIP, FAO-GTOS-TCO, iLEAPS, Max Planck Institute for Biogeochemistry, National Science Foundation, University of Tuscia, Université Laval and Environment Canada, US Department of Energy and NOAA ESRL, as well as many local funders. The authors thank Dr. F. Chevallier for providing the Bayesian model inversion results. Funding for this study was provided by the NASA Earth Science program (NNX11AD46G).

## References

- Adler R F, Gu G and Huffman G J 2012 Estimating Climatological Bias Errors for the Global Precipitation Climatology Project (GPCP) *J. Appl. Meteor. Climatol.* 51 84-99
- Angert A, Biraud S, Bonfils C, Henning C C, Buermann W, Pinzon J, Tucker C J and Fung I 2005 Drier summers cancel out the CO<sub>2</sub> uptake enhancement induced by warmer springs *Proc. Natl. Acad. Sci. U.S.A.* 102 10823-10827
- Baldocchi D 2008 Breathing of the terrestrial biosphere: lessons learned from a global network of carbon dioxide flux measurement systems *Aust. J. Bot.* 56 1-26
- Beck P S and Goetz S J 2011 Satellite observations of high northern latitude vegetation productivity changes between 1982 and 2008: ecological variability and regional differences *Environ. Res. Lett.* 6 045501

- Boesch H, Baker D, Connor B, Crisp D and Miller C 2011 Global characterization of CO<sub>2</sub> column retrievals from shortwave-infrared satellite observations of the Orbiting Carbon Observatory-2 mission *Remote Sensing* 3 270-304
- Bond-Lamberty B, Peckham S D, Ahl D E and Gower S T 2007 Fire as the dominant driver of central Canadian boreal forest carbon balance *Nature* 450 89-92
- Brown R D and Brasnett B 2010 Canadian Meteorological Centre (CMC) Daily Snow Depth Analysis Data, National Snow and Ice Data Center Environmental Canada
- Buermann W, Bikash P R, Jung M, Burn D H, and Reichstein M 2013 Earlier springs decrease peak summer productivity in North American boreal forests *Environ. Res. Lett.* 8 024027
- Chevallier F *et al* 2010 CO<sub>2</sub> surface fluxes at grid point scale estimated from a global 21 year reanalysis of atmospheric measurements *J. Geophys. Res.* 115 D21307
- Davidson E A, Belk E and Boone R D 1998 Soil water content and temperature as independent or confounded factors controlling soil respiration in a temperate mixed hardwood forest *Glob. Change Biol.* 4 217-227
- Desai A R, Helliker B R, Moorcroft P R, Andrews A E and Berry J A 2010 Climatic controls of interannual variability in regional carbon fluxes from top-down and bottom-up perspectives *J. Geophys. Res.* 115 G02011
- Dong J, Walker J P and Houser P R 2005 Factors affecting remotely sensed snow water equivalent uncertainty *Remote Sens. Environ.* 97 68-82
- Entekhabi D *et al* 2010 The Soil Moisture Active Passive (SMAP) mission *Proceedings of the IEEE* 98 704-716

- Friedl M A, Sulla-Menashe D, Tan B, Schneider A, Ramankutty N, Sibley A and Huang X 2010  
MODIS Collection 5 global land cover: Algorithm refinements and characterization of  
new datasets *Remote Sens. Environ.* 114 168-182
- GLOBALVIEW-CO<sub>2</sub> 2012 Cooperative Atmospheric Data Integration Project - Carbon Dioxide  
NOAA ESRL, Boulder, Colorado [Available at  
<http://www.esrl.noaa.gov/gmd/ccgg/globalview/>]
- Goulden M *et al* 1998 Sensitivity of boreal forest carbon balance to soil thaw *Science* 279 214-  
217
- Graven H *et al* 2013 Enhanced seasonal exchange of CO<sub>2</sub> by northern ecosystems since 1960  
*Science* 341 1085-1089
- Gurney K R, Baker D, Rayner P and Denning A S 2008 Interannual variations in regional net  
carbon exchange and sensitivity to observing networks estimated from atmospheric CO<sub>2</sub>  
inversions for the period 1979 to 2006 *Glob. Biogeochem. Cycles* 22 GB3025
- Gurney K R, Chen Y H, Maki T, Kawa S R, Andrews A and Zhu Z 2005 Sensitivity of  
atmospheric CO<sub>2</sub> inversions to seasonal and interannual variations in fossil fuel  
emissions *J. Geophys. Res.* 110 D10308
- Harris I, Jones P D, Osborn T J and Lister D H 2013 Updated high-resolution grids of monthly  
climatic observations – the CRU TS3.10 Dataset *Int. J. Climatol.* doi: 10.1002/joc.3711
- Jones L A and Kimball J S 2010 Daily Global Land Surface Parameters Derived from AMSR-E,  
Boulder Colorado USA: National Snow and Ice Data Center. Digital media  
(<http://nsidc.org/data/nsidc-0451.html> )

- Jones L A, Kimball J S, McDonald K C, Chan S K, Njoku E G and Oechel W C 2007 Satellite microwave remote sensing of boreal and Arctic soil temperatures from AMSR-E *IEEE Trans. Geosci. Remote Sens.* 45 2004-2018
- Kim Y, Kimball J S, Zhang K and McDonald K C 2012 Satellite detection of increasing Northern Hemisphere non-frozen seasons from 1979 to 2008: Implications for regional vegetation growth *Remote Sens. Environ.* 121 472-487
- Kurz W A, Dymond C C, Stinson G, Rampley G J, Neilson E T, Carroll A L, Ebata T and Safranyik L 2008 Mountain pine beetle and forest carbon feedback to climate change *Nature* 452 987-990
- Lupascu M, Welker J M, Seibt U, Maseyk K, Xu X and Czimczik C I 2013 High Arctic wetting reduces permafrost carbon feedbacks to climate warming *Nature Climate Change* 4 51-55
- Masarie K A and Tans P P 1995 Extension and Integration of Atmospheric Carbon Dioxide Data into a Globally Consistent Measurement Record *J. Geophys. Res.* 100 11593-11610
- McGuire A D *et al* 2012 An assessment of the carbon balance of arctic tundra: Comparisons among observations, process models, and atmospheric inversions *Biogeosciences* 9 3185-3204
- Nemani R, Keeling C, Hashimoto H, Jolly W, Piper S, Tucker J C, Myneni R and Running S W 2003 Climate-driven increases in global terrestrial net primary production from 1982 to 1999 *Science* 300 1560-1563
- Olivas P C, Oberbauer S F, Tweedie C E, Oechel W C and Kuchy A 2010 Responses of CO<sub>2</sub> flux components of Alaskan Coastal Plain tundra to shifts in water table *J. Geophys. Res.* 115 G00I05

- Peters W *et al* 2007 An atmospheric perspective on North American carbon dioxide exchange: CarbonTracker *Proc. Natl. Acad. Sci. U.S.A.* 104 18925-18930
- Piao S *et al* 2008 Net Carbon dioxide losses of northern ecosystems in response to autumn warming *Nature* 451 49-52
- Randerson J T, Thompson M V, Conway T J, Fung I Y and Field C B 1997 The contribution of terrestrial sources and sinks to trends in the seasonal cycle of atmospheric carbon dioxide *Glob. Biogeochem. Cycles* 1997 11 535-560
- Smith E A *et al* 2007 International Global Precipitation Measurement (GPM) program and mission: An overview. *Measuring Precipitation from Space: EURAINSAT and the Future* Levizzani V, Bauer P and Turk F J Eds. Springer 611-654
- Solomon S, Qin D, Manning M, Marquis M, Averyt K, Tignor M M B, Miller Jr. H L and Chen Z Eds. 2007 *Climate Change 2007: The Physical Science Basis* Cambridge University Press 996 pp
- Thoning K W, Tans P P and Komhyr W D 1989 Atmospheric carbon dioxide at Mauna Loa Observatory, 2. Analysis of the NOAA/GMCC data, 1974-1985 *J. Geophys. Res.* 94 8549-8565
- Valentini R *et al* 2000 Respiration as the main determinant of carbon balance in European forests *Nature* 404 861-865
- van der Werf G R, Randerson J T, Giglio L, Collatz G J, Mu M, Kasibhatla P S, Morton D C, DeFries R S, Jin Y and van Leeuwen T T 2010 Global fire emissions and the contribution of deforestation, savanna, forest, agricultural, and peat fires (1997-2009) *Atmos. Chem. Phys.* 10 11707-11735

- Welp L R, Randerson J T and Liu H P 2007 The sensitivity of carbon fluxes to spring warming and summer drought depends on plant functional type in boreal forest ecosystems *Agric. For. Meteorol.* 147 172-185
- Wunch D *et al* 2013 The covariation of Northern Hemisphere summertime CO<sub>2</sub> with surface temperature in boreal regions *Atmos. Chem. Phys.* 13 9447–9459
- Xu L *et al* 2013 Temperature and vegetation seasonality diminishment over northern lands *Nature Climate Change* 3 581-586
- Yi C *et al* 2010 Climate control of terrestrial carbon exchange across biomes and continents, *Environ Res. Lett.* 5 034007
- Yi Y, Kimball J S, Jones L A, Reichle R H and McDonald K C 2011 Evaluation of MERRA land surface estimates in preparation for the Soil Moisture Active Passive Mission *J. Climate* 24 3797-3816
- Yi Y, Kimball J S, Jones L A, Reichle R H, Nemani R and Margolis H A 2013 Recent climate and fire disturbance impacts on boreal and arctic ecosystem productivity estimated using a satellite-based terrestrial carbon flux model *J. Geophys. Res.* 118 606-622
- Zhang K, Kimball J S, Hogg E H, Zhao M, Oechel W C, Cassano J J and Running S W 2008 Satellite-based model detection of recent climate-driven changes in northern high-latitude vegetation productivity *J. Geophys. Res.* 113 G03033

## Supplement information

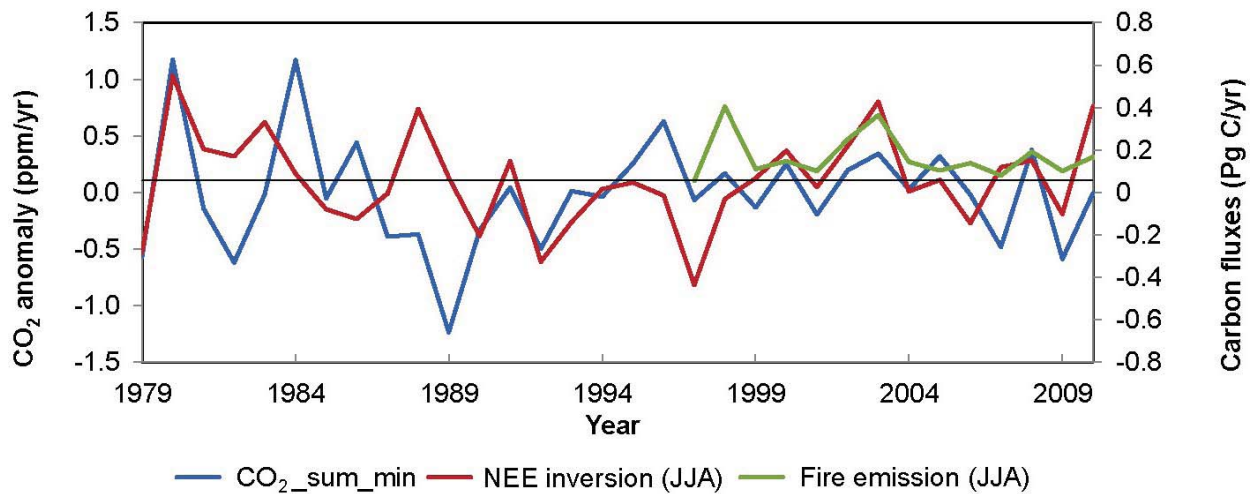


**Fig. S1.** Interannual variability of the northern ( $\geq 50^\circ\text{N}$ ) atmosphere CO<sub>2</sub> summer minimum (CO<sub>2</sub>\_sum\_min, ppm/yr) derived from NOAA MBL reference datasets, atmospheric model inversion estimated summer (JJA) NEE fluxes (Pg C/yr, Chevallier *et al* 2010), and GFED (v.3.1) estimated CO<sub>2</sub> fire emissions (Pg C/yr). Both CO<sub>2</sub>\_sum\_min and NEE inversion estimates were detrended for examining interannual variability. Positive (negative) carbon values denote net ecosystem carbon source (sink) activity.

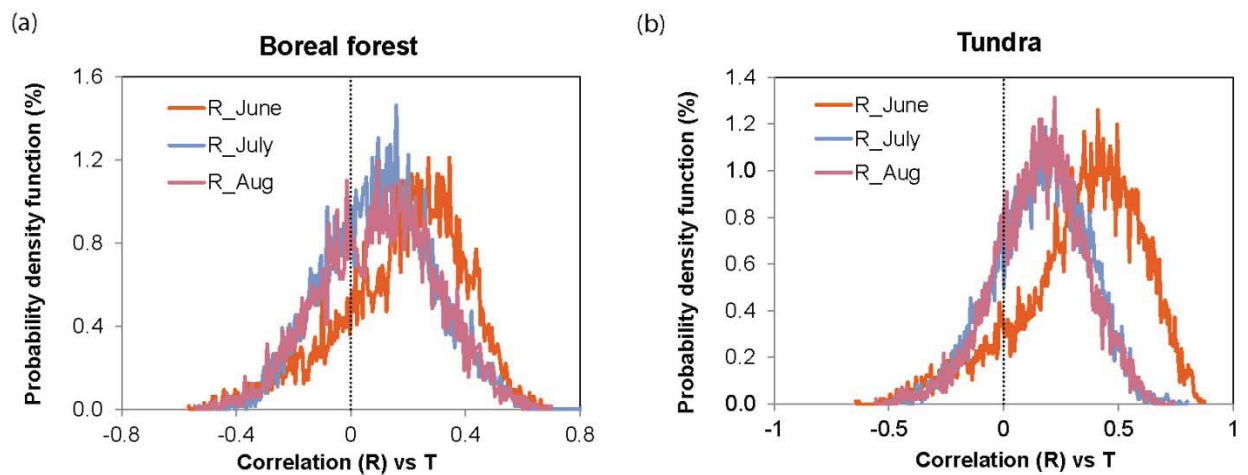


**Fig. S2.** Probability density functions of partial correlation coefficients (R) between GIMMS3g summer (JJA) NDVI and monthly CRU air temperature (T), accounting for the control effects of GPCP precipitation, for boreal forest (a) and tundra (b) classified areas separately for the 1982 to 2010 record. For boreal forest, 29.4%, 13.1% and 14.4% of the pixels show significant ( $p < 0.1$ )

positive correlation with air temperature for June, July and August, respectively. For tundra, 60.5%, 23.7%, and 21.0% of the pixels show significant positive correlation with June, July and August air temperatures. All time series were detrended prior to the correlation analysis.

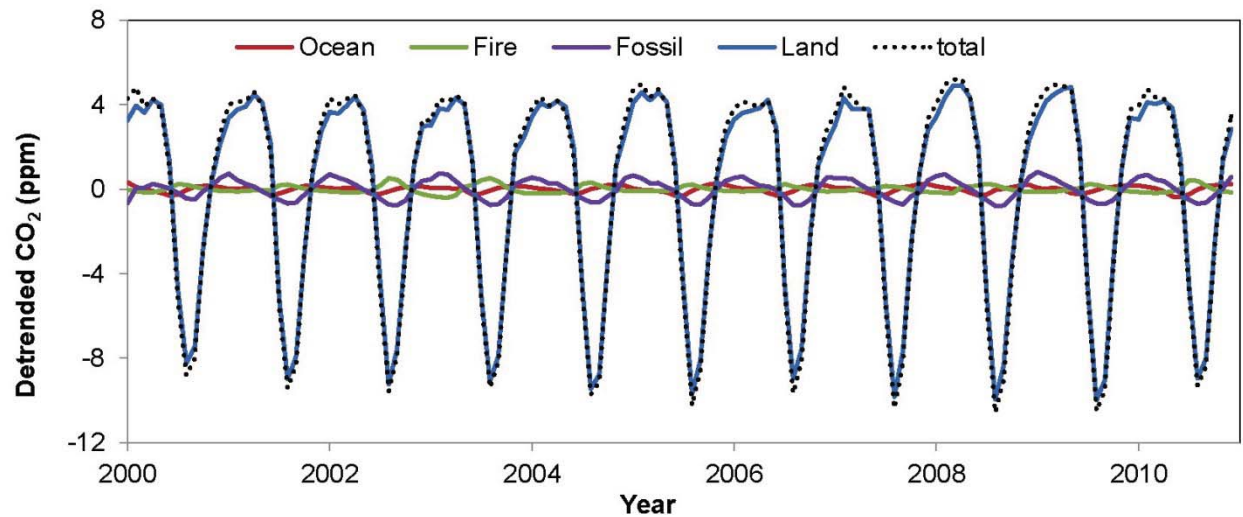


**Fig. S3.** The detrended seasonal cycle of atmospheric CO<sub>2</sub> concentrations contributed by each component of the surface-atmospheric exchange fluxes extracted from atmospheric CO<sub>2</sub> mole fractions simulated by CarbonTracker (2000-2010) in the northern latitudes ( $\geq 50^\circ\text{N}$ ). The CO<sub>2</sub> concentrations (ppm) were simulated using CarbonTracker optimized surface fluxes and an atmospheric transport model (TM5). The surface-atmosphere CO<sub>2</sub> contributions include fossil fuel emissions ('Fossil'), terrestrial biosphere fluxes excluding fire, i.e. NEE ('Land'), fire emissions ('Fire'), and air-sea gas exchange ('Ocean'). The total CO<sub>2</sub> concentration is the sum of the four components.

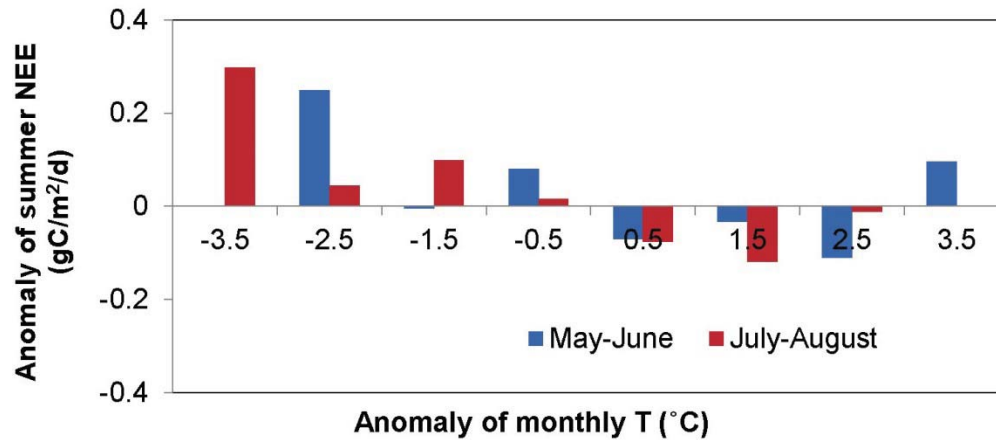


**Fig. S4.** Tower eddy covariance measurement based estimates of summer NEE anomalies ( $\text{g C/m}^2/\text{d}$ ) for four boreal sites (Table S6) in northern Europe. The anomalies of tower measured summer (JJA) NEE fluxes are shown in relation to growing-season (from May to August) anomalies of monthly air temperature binned into  $1.0\text{ }^\circ\text{C}$  intervals. There are 20 site-years for each month from May to August. The analysis period is divided into early growing-season (May-June) and later growing-season (July-August). Summer NEE is generally negatively correlated with growing-season (May to August) air temperature, with significant ( $p < 0.05$ ) correlations for June and August. There are few in situ soil moisture records for each month ( $\sim 10$  records, not shown), which show a weak ( $p > 0.1$ ) positive correlation with summer NEE, likely due to a strong negative correlation ( $p < 0.05$ ) between air temperature and soil moisture at those sites.

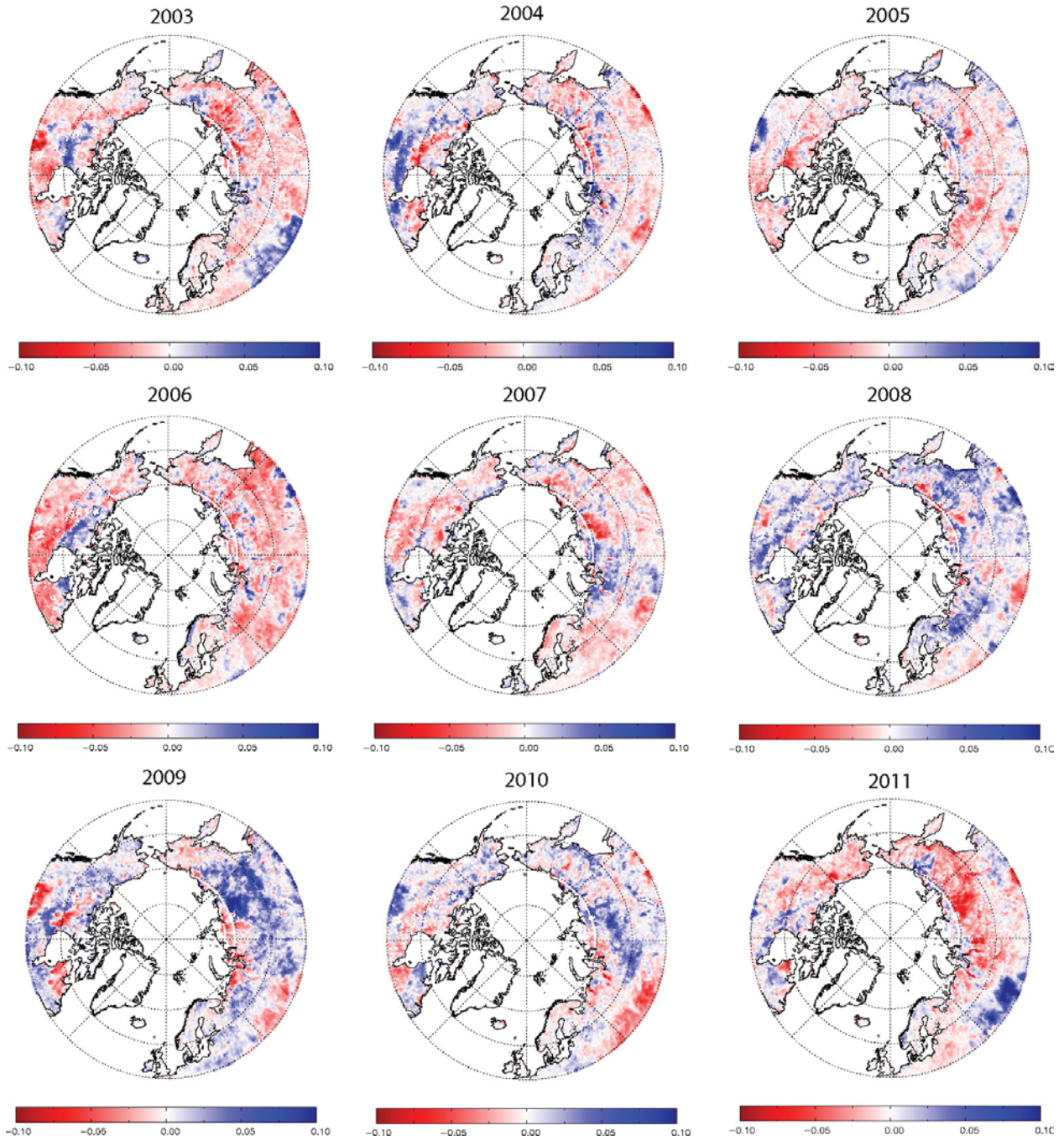


**Fig. S5.** Spatial pattern of detrended AMSR-E surface ( $\leq 2\text{cm}$ ) soil moisture ( $\text{m}^3/\text{m}^3$ ) in June from 2003 to 2011.

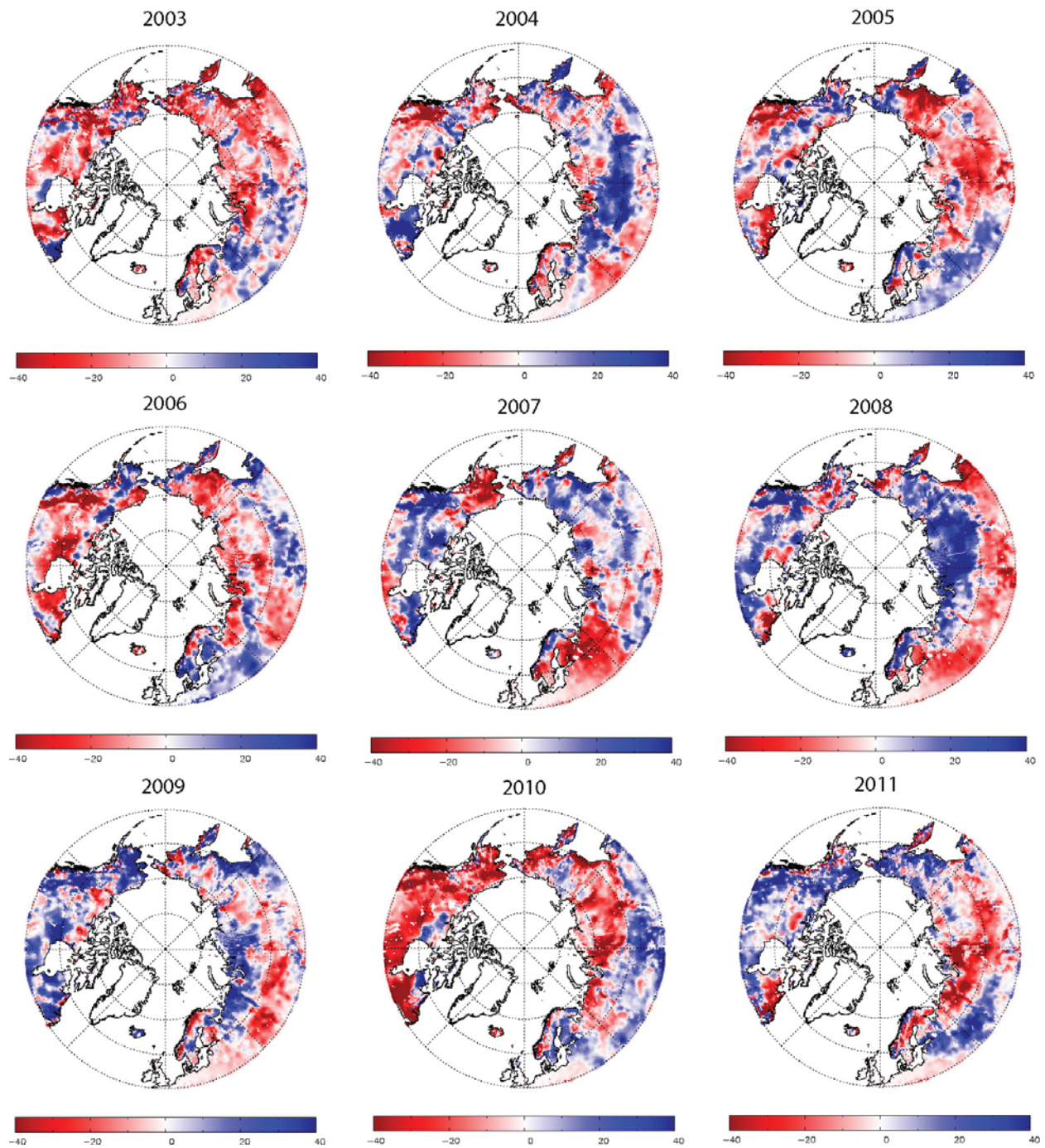


**Fig. S6.** Spatial pattern of detrended CMC spring (MAM) SWE (mm) from 2003 to 2011.

**Table S1.** The nine atmospheric CO<sub>2</sub> MBL flask sites ( $\geq 50$  °N) used in Fig. 1 (b).

Sites	Lon (°)	Lat (°)	Period <sup>1</sup>
ALT	-62.51	82.45	1989-2010
Zep	11.89	78.91	2000-2009
MBC	-119.35	76.25	1981-1996
BRW	-156.61	71.32	1979-2010
STM	2.00	66.00	1982-2008
ICE	-20.29	63.40	2003-2010
CBA	-162.72	55.20	1979-1996
MHD	-9.90	53.33	1992-2010
SHM	174.13	52.71	1995-2004

<sup>1</sup>The period may be shorter when analyzing the correlation between summer CO<sub>2</sub> minimum and CMC SWE (only available from 1999 to 2011).

**Table S2.** Flux tower sites located in boreal ( $\geq 50$  °N) NA and northern Eurasia used in Fig. 3. Only sites with 2 or more years of daily carbon fluxes and extending over at least part of the growing season (May to August) were selected for the analysis. A total of 23 sites were used for this study, with relatively few sites in northern Eurasia.

Site name	Latitude (°)	Longitude (°)	Biome <sup>1</sup>	Climate
CA-Oas	53.63	-106.20	4	Boreal
CA-Obs	53.99	-105.12	1	Boreal
CA-Ojp	53.92	-104.69	1	Boreal
CA-SF1	54.48	-105.82	1	Boreal
CA-SF2	54.25	-105.88	1	Boreal
CA-SF3	54.09	-106.00	1	Boreal
CA-SJ1	53.91	-104.66	1	Boreal
CA-SJ2	53.94	-104.65	1	Boreal
CA-SJ3	53.88	-104.64	1	Boreal
CA-WP1	54.95	-112.47	5	Boreal
CA-Man	55.88	-98.48	1	Boreal
CA-NS1	55.88	-98.48	1	Boreal
CA-NS2	55.90	-98.52	1	Boreal
CA-NS4	55.91	-98.38	1	Boreal
CA-NS5	55.86	-98.48	1	Boreal
CA-NS7	56.64	-99.95	7	Boreal
US-Atq	70.47	-157.41	11	Arctic
US-Ivo	68.49	-155.75	11	Arctic
US-Brw	71.32	-156.63	11	Arctic
RU-Zot	60.81	89.35	1	Boreal
RU-Che	68.61	161.34	5	Boreal
RU-Ha1	54.72	90.00	10	Boreal

RU-Cok	70.62	147.88	7	Boreal
--------	-------	--------	---	--------

<sup>1</sup>: 1: Evergreen needle-leaf forest, 4: Deciduous broadleaf forest, 5: Mixed forest, 7: Shrublands, 10: Grasslands, 11: Wetland.

**Table S3.** The highest partial correlation (R) of summer net carbon uptake indicated by CO<sub>2</sub>\_sum\_min derived from MBL reference datasets and atmospheric model inversion estimated regional mean NEE (Chevallier *et al* 2010) versus the regional climate variables during the period varying from January to August, and for the 1979 to 2010 record for the northern latitudes ( $\geq 50^{\circ}\text{N}$ ). The climate variables include precipitation (P), air temperature (T) and snow water equivalent (SWE). For the partial correlation analysis against P and SWE, T was used as the controlling variable; for partial correlation analysis against T, P was used as the controlling variable. All time series were detrended prior to examining annual anomalies. Significant correlations are indicated in bold.

	CO <sub>2</sub> _sum_min	NEE (summer)
R vs. P	<b>-0.57**</b> (Jan-May)	<b>-0.33*</b> (Feb-April)
R vs. T	0.26 (Jan-Mar)	<b>0.52**</b> (Jul-Aug)
R vs. SWE (CMC) <sup>1</sup>	<b>-0.51*</b> (Feb)	<b>-0.51*</b> (Apr-May)

\*p<0.1; \*\*p<0.05

<sup>1</sup>CMC data only available from 1999 to 2011.

**Table S4.** Correlation coefficient (R) of summer (JJA) NEE anomalies versus in situ monthly air temperature (T) and surface ( $\leq 15$  cm) soil water content (SWC1) anomalies during the growing season (May-September) for boreal NA and Eurasian EC tower sites (Table S2). Summer NEE is significantly (p<0.1) positively correlated with monthly air temperature and negatively correlated with monthly SWC1 during the growing season following removal of two anomalous CA-Oas summer NEE outliers with R values shown in parentheses. During the soil thawing period (April and May), surface soil moisture is positively correlated with air temperature, while surface soil moisture is negatively correlated with air temperature during the later growing season (i.e. July and August) due to enhanced evaporation. The number of site data records used for this analysis varies from month to month, with generally more available air temperature measurements than soil moisture measurements.

	May	June	July	August
T vs NEE	0.25 (0.45**)	0.22 (0.52**)	0.10 (0.38**)	0.26* (0.53**)
SWC1 vs NEE	-0.52** (-0.35*)	-0.51** (-0.59**)	-0.26 (-0.46**)	-0.14 (-0.37*)

T vs SWC1	0.32*	-0.26 (p=0.10)	-0.39**	-0.33*
-----------	-------	----------------	---------	--------

\* P<0.1; \*\* p<0.05

**Table S5.** Available flux tower sites located in boreal ( $\geq 50$  °N) Europe. Most of the flux tower sites in Europe are located in temperate climate areas, and only sites in the boreal climate zone (4) were included in this study (below).

Site name	Latitude (°)	Longitude (°)	Biome <sup>1</sup>	Climate
FI-Kaa	69.14	27.30	11	Boreal
SE-Fla	64.11	19.46	1	Boreal
FI-Hyy	61.85	24.29	1	Boreal
FI-Sod	67.36	26.64	1	Boreal

<sup>1</sup>Same as Table S2.